

Quantitative Detection of Photothermal and Photoelectrocatalytic Effects Induced by SPR from Au@Pt Nanoparticles

Hao Yang, Lan-Qi He, Yu-Wen Hu, Xihong Lu, Gao-Ren Li, Biju Liu, Bin Ren,*
Yexiang Tong,* and Ping-Ping Fang*

Abstract: The surface plasmon resonance (SPR) induced photothermal and photoelectrocatalysis effects are crucial for catalytic reactions in many areas. However, it is still difficult to distinguish these two effects quantitatively. Here we used surface-enhanced Raman scattering (SERS) to detect the photothermal and photoelectrocatalytic effects induced by SPR from Au core Pt shell Nanoparticles (Au@Pt NPs), and calculated the quantitative contribution of the ratio of the photothermal and photoelectrocatalysis effects towards the catalytic activity. The photothermal effect on the nanoparticle surface after illumination is detected by SERS. The photoelectrocatalytic effect generated from SPR is proved by SERS with a probe molecule of *p*-aminothiophenol (PATP).

Efficient harvesting of solar energy has been a worldwide priority target.^[1] Surface plasmon resonance (SPR) can create sharp spectral absorption and scattering peaks as well as strong electromagnetic near-field enhancements when coupling with metal nanostructures under irradiation.^[2] Excited plasmon resonances can greatly enhance the electric field near the nanocrystal surface as well as the catalytic activity.^[3] Therefore, the investigation of the SPR induced photothermal and photoelectrocatalysis effects are important to understand the mechanisms for the catalytic reactions.

Plasmonic effect can shift the absorption to the visible light region, which facilitates the conversion of solar energy to chemical energy over photocatalysts. SPR induced photocatalysis is especially important because it is the direct interactions between the plasmonic nanocrystals and the reactive molecules.^[4] A possible way for this interaction is directly injecting the excited hot electrons from plasmonic nanocrystals into the antibonding orbitals of adsorbed molecules.^[5] The occupation of the antibonding orbitals will

weaken the related bonds and lead to desired reactions. Plasmonic photocatalysis has been reported to drive the oxidation of formaldehyde and methanol by Au nanocrystals.^[6] Plasmon resonance has also been reported to enhance the catalytic activity of the Suzuki coupling reactions,^[7] the hydrogen generation reactions,^[8] and other reactions.^[9] During these processes, the plasmonic photothermal and photoelectrocatalytic conversion can be employed to enhance the chemical reactions. However, the quantitative measurement of the photothermal and photoelectrocatalytic activities induced by SPR has remained elusive.

The temperature measurements on the hot nanoparticles (NPs) surfaces are very important for the mechanism studies of the catalytic reactions. Many efforts have been made to develop lots of techniques to measure the temperature of the hot spot of the NPs surface.^[10] Takase et al. has found that there is a shift in the wavenumber depending on the illuminated laser power density in SERS.^[11] Neumann et al. has used SPR of the nanoparticle to heat the aqueous solution and make steam.^[12] Besides the temperature, it is even more difficult to prove the photoelectrocatalytic process induced by SPR. Huang et al. has proved by SERS that oxygen molecules could be activated by accepting an electron from Au nanoparticle under the excitation of SPR to form a strongly adsorbed oxygen molecule anion.^[13] However, whether such oxygen activation can happen on transition metals to enhance the catalytic activity is still unclear. Therefore, further efforts are needed to study the photoelectrocatalytic activity induced by SPR.

In this work we quantitatively calculated the contribution ratios of the photothermal and photoelectrocatalytic effects induced by SPR to catalytic reactions. We take advantage of the plasmonic Au core with strong SPR to enhance the catalytic activity under illumination by the Au core Pt cluster NPs (Au@Pt NPs). SERS is used to detect the photothermal and photoelectrocatalytic effects induced by SPR. SERS is used to detect the photothermal effect, while the probe molecule of *p*-aminothiophenol (PATP) is used to investigate the photoelectrocatalytic effect. The contribution ratios of the photothermal and photoelectrocatalytic effects are calculated according to the catalytic activity and SERS results.

A key issue in this study was the dependence of the catalytic activity on the SPR effect. To study the SPR enhanced catalytic activity, we used cyclic voltammetry (CV) to systemically investigate the influence of the illuminating time on the catalytic activity of the 55 nm Au@2Pt and Au@20Pt NPs (with a Au core of about 55 nm and 2 or 20 equivalent monolayers of Pt according to the calculation) on fluorine-doped tin oxide (FTO) in 0.5 M methanol + 1 M

[*] H. Yang, L. Q. He, Y. W. Hu, Dr. X. Lu, Prof. G. R. Li, Prof. Y. Tong, Dr. P. P. Fang
KLGHEI of Environment and Energy Chemistry
MOE of the Key Laboratory of Bioinorganic and Synthetic Chemistry
School of Chemistry and Chemical Engineering
Sun Yat-Sen University, Guangzhou 510275 (China)
E-mail: fangpp3@mail.sysu.edu.cn
chedhx@mail.sysu.edu.cn

Dr. B. Liu, Prof. B. Ren
State Key Laboratory of Physical Chemistry of Solid Surfaces,
Collaborative Innovation Center of Chemistry for Energy Materials,
College of Chemistry and Chemical Engineering, Xiamen University
Xiamen 361005 (China)
E-mail: bren@xmu.edu.cn



Supporting information for this article is available on the WWW under <http://dx.doi.org/10.1002/anie.201505985>.

NaOH, and the experiment details are in S1 in the supporting information (SI). It is important to note that Pt was grown on Au as a set of clusters and not as a set of consecutive monolayers; however, here we will use monolayer-equivalents as a convenient method for describing the amount of Pt added to each nanoparticle. As the 55 nm Au NPs have the SPR peak at ca. 530 nm, a wavelength of 530 ± 10 nm light with a power density of 10 mW cm^{-2} was used as the illumination light. With the increase of the illuminating time, the catalytic activity increases gradually until 25 min and then keeps constant (Figure 1A). The Au@2Pt NPs, which have strong absorption at ca. 530 nm due to the SPR effect and weak peak at about 750 nm because of the plasmon coupling between nanoparticles (Figure 1B), exhibit ca. 2.6 times enhancement in catalytic activity after illumination for 25 min. In contrary, owing to the blocked SPR effect as a result of the thick Pt coverage (Figure 1C), the Au@20Pt NPs have very weak absorption at ca. 530 nm, and therefore exhibit weaker enhancement in catalytic activity than the Au@2Pt NPs after illumination (Figure 1D).

In order to further prove that such remarkably enhanced catalytic activity after illumination was caused by SPR, we changed the illumination wavelength from the SPR peak at ca. 530 nm to ca. 630 nm light. The power density of each illumination wavelength on the sample is 10 mW cm^{-2} . A drastic decrease in catalytic activity was found when changing the illumination wavelength from 530 ± 10 nm to 630 ± 10 nm (Figure 1E). This is because the SPR effect of the 55 nm Au@2Pt NPs is strong at ca. 530 nm and weak at ca. 630 nm,

and therefore they exhibit higher catalytic activity when illuminating at 530 ± 10 nm than at 630 ± 10 nm (Figure 1E). We also found that the white and ultraviolet light with the same power density were not as efficient as the 530 nm light because of the SPR effect (see S2 in the SI). We also eliminated the SPR effect completely to make sure the SPR enhanced catalytic activity with Pd@2Pt nanocubes that have no SPR. We found there was a very weak catalytic activity enhancement after illumination (see S3 in the SI). Therefore, such enhanced catalytic activity is caused by the SPR effect from the Au core.

The harvesting of light energy using SPR from Au nanocrystal cores to enhance the catalytic activity of chemical reactions has attracted great interest. Wang et al. has used the Au core to enhance the catalytic activity for the Suzuki coupling reaction from the Pd shell.^[7a] They found that both plasmonic photoelectrocatalysis and photothermal heating induced by SPR contribute to the catalytic activity of the Suzuki coupling reaction. Zheng et al. has also used Pt-modified Au nanorods (NRs) to enhance the catalytic activity of the hydrogen generation reaction.^[8,14] They found that the Pt-tipped Au NRs exhibited efficient photocatalytic H_2 evolution under visible and near-infrared light because the hot electrons arose from the excitation of surface plasmons in Au NRs. However, the quantitative calculation of the catalytic activity contribution from the plasmonic photo-thermal and photoelectrocatalytic is still unclear.

Therefore, we did further experiments to distinguish the photothermal and photoelectrocatalytic effects on the enhanced catalytic activity. We tried to measure the photothermal effect by SERS first. The direct detection of the temperature on the NPs surface instead of the bulk solution is very essential for the mechanism analysis in the catalytic reactions. SERS is a powerful tool that can be used for in situ studies, and therefore we can detect the surface temperature of the NPs in situ by taking advantages of SERS according to the method of Ren and co-workers.^[15] The details for measuring the temperature of the hot NPs are shown in S4 in the SI. We found that the temperature of the hot Au@2Pt NPs surface increased from 23 to about 80°C when illuminating with the ca. 530 nm light from 0 min to 25 min with a power density of 10 mW cm^{-2} , and then kept constant, which is similar as in the literature.^[16] When the power density of 30 mW cm^{-2} was illuminating on the Au@2Pt NPs for 25 min, the temperature increased to 95°C . The temperature of the Au@20Pt NPs surface increased from 23 to about 40°C when illuminating from 0 min to 25 min and then kept constant. This is one of the reasons why the catalytic activity for the Au@2Pt NPs is higher than that for the Au@20Pt NPs.

After knowing the temperature of the hot NPs surface, we then systematically investigated the dependence of the catalytic activity on the temperature by the i - t curve. The temperature was controlled by the water bath. As shown in Figure 2, the catalytic activity would increase gradually as the temperature increases. As detected by SERS, the final temperature for the Au@2Pt NPs after 25 min illumination with 10 mW cm^{-2} under 530 nm light was around 80°C , however, the catalytic activity for the Au@2Pt NPs under illumination was higher than the catalytic activity in 80°C

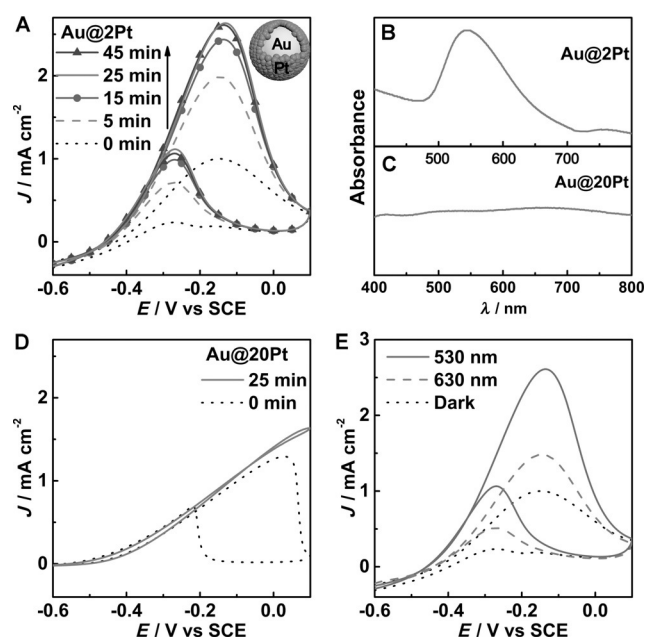


Figure 1. CV of 55 nm Au@2Pt NPs (A) and 55 nm Au@20Pt NPs (D) in a solution of 0.5 M methanol + 1 M NaOH with different illumination time under 530 ± 10 nm light with a power density of 10 mW cm^{-2} ; UV-Vis absorption spectra of 55 nm Au@2Pt NPs (B) and 55 nm Au@20Pt NPs (C) on FTO. CV of 55 nm Au@2Pt NPs with different illuminating bandpass filter with a power density of 10 mW cm^{-2} for 25 min in a solution of 0.5 M methanol + 1 M NaOH (E). The scanning rate was 50 mV s^{-1} .

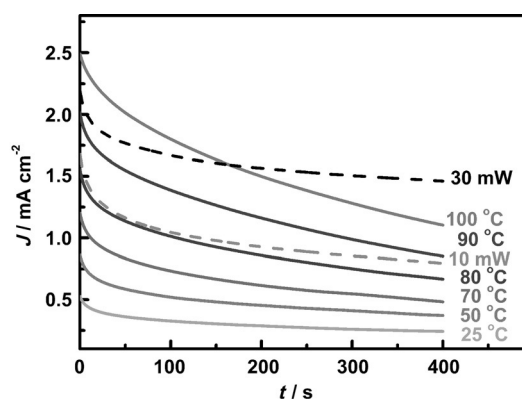


Figure 2. *i*–*t* curves for 55 nm Au@2Pt NPs in different temperature solution and under illumination with different power density of 530 ± 10 nm light. All these experiments were carried out in a 0.5 M methanol + 1 M NaOH solution at -0.25 V for 400 s.

solution (Figure 2). More interestingly, the catalytic activity for the Au@2Pt NPs after 25 min illumination with 30 mW cm^{-2} under 530 nm light was higher than that in the 90°C or even 100°C solution (Figure 2). The current density under illumination is more stable than controlling the temperature. We did five groups of the experiments to confirm these results (see S5 in the SI). Therefore, besides the photothermal effect, the photoelectrocatalytic effect should exist during the catalytic reaction.

We then used SERS to prove the photoelectrocatalytic effect during the catalytic reaction. Similar as in the photothermal effect investigated by SERS, a probe molecule of PATP was used to detect the photoelectrocatalytic effect. The bands of a_g at 1140, 1388 and 1434 cm^{-1} appeared after illumination with laser means that PATP was oxidized to *p,p'*-dimercaptoazobenzene (DMAB).^[13] When PATP adsorbed on the Au@2Pt NPs surface with air, the a_g mode appeared (Figure 3A), which indicates the selective oxidation from PATP to DMAB happened in air. The selective oxidation reaction cannot happen in N_2 atmosphere because it has no oxygen to oxidize PATP. However, when PATP adsorbed on

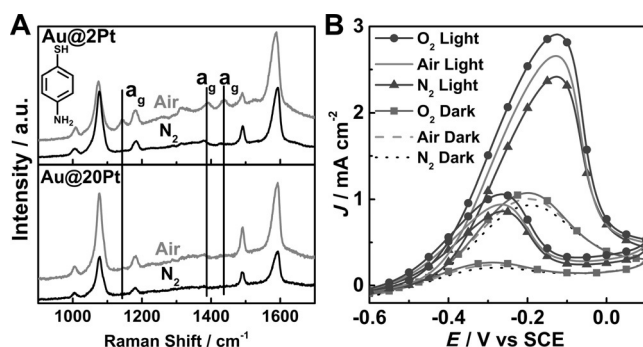


Figure 3. SERS spectra of PATP adsorbed on Au@2Pt NPs and Au@20Pt NPs in N_2 and air with a power of about 0.6 mW on the sample (A); CV of 55 nm Au@2Pt NPs saturated with N_2 , air and O_2 in a solution of 0.5 M methanol + 1 M NaOH with and without illumination under 530 ± 10 nm light with a power density of 10 mW cm^{-2} for 25 min (B). The scanning rate was 50 mV s^{-1} .

the Au@20Pt NPs surface, the selective oxidation from PATP to DMAB was not observed in air (Figure 3A). This is because the SPR of the Au@20Pt NPs are dramatically blocked by the thick Pt cluster, and therefore the selective oxidation from PATP to DMAB happens only on the Au@2Pt NPs in air. Additionally, PATP cannot be oxidized to DMAB in air at high temperature (see S6 in the SI). The selective oxidation from PATP to DMAB happens because the SPR can excite the electrons and results in electron transfer from NPs to $^3\text{O}_2$ in air to yield $^2\text{O}_2^-$,^[13] which can strongly adsorb on the surface of the NPs and facilitate the selective oxidation of PATP to DMAB. If the SPR is blocked, such hot electron is difficult to transfer.^[4b] Therefore, we can deduce that the oxygen can be activated by the SPR on the Au@2Pt NPs but cannot on the Au@20Pt NPs. Such electron transfer may also facilitate the electrooxidation of methanol, which can enhance the catalytic activity.

In order to prove such catalytic enhancement, the electrooxidation activities of methanol in N_2 , air and O_2 saturated solution with and without illumination were measured for comparison. The current density from dark to illumination increased from 0.93, 1.01 and 1.07 to 2.41, 2.66 and 2.91 mA cm^{-2} in N_2 , air and O_2 atmosphere, respectively. The current density increased about 2.59, 2.63, 2.71 times from dark to illumination in N_2 , air and O_2 (Figure 3B). Five groups of the experiments showed the same trend (see S7 in the SI). The further catalytic activity enhancement in O_2 reveals that O_2 has been activated during the illumination. This confirmed with the SERS results in Figure 3A that O_2 was activated by the surface plasmon, as in the literature.^[13] The resulting electron transfer from NPs to $^3\text{O}_2$ in air to yield $^2\text{O}_2^-$ is due to the SPR effect from the Au core, which is the reason why the SPR can enhance the photoelectrocatalytic activity.^[13] The increased catalytic activity for the Au@2Pt NPs in N_2 is attributed to the photothermal effect while in O_2 is caused by both the photothermal and photoelectrocatalytic effects. Therefore, the SPR-assisted activation of oxygen on Au@2Pt NPs contributes to the enhanced catalytic activity of the methanol electrooxidation. This is also may be one of the reasons why the catalytic activity increased much more after illumination for the Au@2Pt NPs than for the Au@20Pt NPs, and further mechanism studies are undergoing in our labs.

We have confirmed that the enhanced catalytic activity induced by SPR is caused by the photothermal and photoelectrocatalytic effects, but the quantitative calculation of the catalytic activity contribution is still a great challenge. Here we chose the *i*–*t* curves at 25°C and 80°C in Figure 2 to calculate the quantitative contribution of the photothermal and photoelectrocatalytic effects induced by SPR. When the *i*–*t* curves went to 200 seconds, the light was switched on and an immediate increase of the current was observed (Figure 4). The current before switching on the light at 200 seconds was designed as i_0 , while the current after immediate illumination was designed as i_1 . The 20 seconds' illumination made no obvious increase of the temperature on the nanoparticle surface according to SERS experiment (see S8 in the SI), and therefore the immediate increase of the current after illumination was contributed by the photoelectrocatalytic effect. The contribution ratio for the photoelectrocatalytic

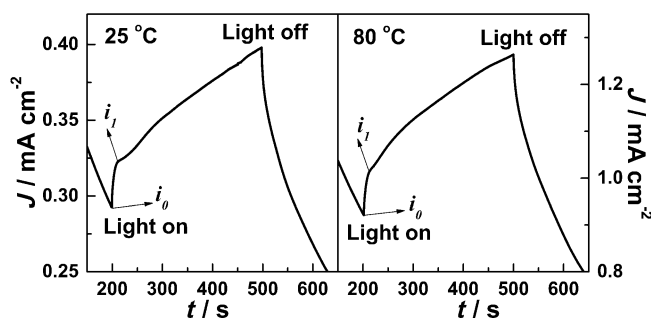


Figure 4. i - t curves for 55 nm Au@2Pt NPs under 530 ± 10 nm light with a power density of 10 mW cm^{-2} in a 0.5 M methanol + 1 M NaOH solution at 25 and 80 °C at -0.25 V for 700 s.

effect would be $(i_1 - i_0)/i_1$. The contribution ratio for the photoelectrocatalytic effect was calculated to be about $10 \pm 2\%$ for the Au@2Pt NPs at 25 and 80 °C for 10 groups of samples. After about 20 seconds illumination, the current began to increase as a result of the gradual increase of the temperature due to the photothermal effect from the illumination. The immediate current increase during the first 10 seconds after illumination for the i - t curve at 25 °C or 80 °C is similar, however, the current density increased faster during the 20 to 50 seconds for the 80 °C than the 25 °C in the i - t curve because of the lower temperature difference, which also means that the immediate current increase was caused by the photoelectrocatalytic effect. When the light was turned off at 500 seconds, an immediate decrease of the current was observed because of the photoelectrocatalytic effect and a gradual decrease of the current because of the photothermal effect (Figure 4). This method combining SERS and catalytic activity together can be used to calculate the contribution ratios of the photothermal and photoelectrocatalytic effect induced by SPR for other reactions as well.

In conclusion, we have distinguished the photothermal and photoelectrocatalytic effects enhanced by the SPR catalytic activity using SERS. Benefiting from the photothermal and photoelectrocatalytic effects from SPR, the catalytic activity of the Au@2Pt NPs can be enhanced by about 2.6 times under illumination with 530 nm light. The real temperature on the hot Au@2Pt NPs surface is measured to be about 80 and 95 °C after illuminating with 530 ± 10 nm light for 25 min with a power density of 10 mW cm^{-2} and 30 mW cm^{-2} by SERS, which would be a very important method for in situ temperature studies of catalytic reaction on the hot NPs surface in the future. The selective oxidation of PATP to DMAB induced by SPR has proven that the photoelectrocatalytic effect was presented on the Au@2Pt NPs. Although the final temperature after illuminating with 30 mW cm^{-2} for 25 min under 530 nm light is about 95 °C, the final current density is higher than that for the 100 °C solution, which further confirms the photoelectrocatalytic effect during the catalytic reaction. The quantitative contribution to the catalytic activity from the photothermal and photoelectrocatalytic effects induced by SPR is calculated from the i - t curves when switching on the light, which is about 90% for the photothermal effect and 10% for the photoelectrocatalytic effect. The photothermal and photoelectrocatalytic effects

induced by SPR can be used to enhance other reactions and such method can provide great facility to investigate the mechanism in the future studies.

Acknowledgements

This work was supported by the Natural Science Foundations of China (Grant Nos. 21405182, 21476271, 21461162003 and 21403306). We also thank the Young Teacher Starting-up Research, the Laboratory opening Fund of Sun Yat-Sen University and the Ministry of education personnel returning from overseas funds.

Keywords: heterogeneous catalysis · photoelectrocatalysis · photothermal · surface plasmon resonance · surface-enhanced raman scattering

How to cite: *Angew. Chem. Int. Ed.* **2015**, *54*, 11462–11466
Angew. Chem. **2015**, *127*, 11624–11628

- [1] a) X. Z. Li, F. B. Li, *Environ. Sci. Technol.* **2001**, *35*, 2381–2387; b) T. P. Yoon, M. A. Ischay, J. N. Du, *Nat. Chem.* **2010**, *2*, 527–532; c) O. K. Varghese, M. Paulose, T. J. LaTempa, C. A. Grimes, *Nano Lett.* **2009**, *9*, 731–737.
- [2] a) S. Yu, Y. H. Kim, S. Y. Lee, H. D. Song, J. Yi, *Angew. Chem. Int. Ed.* **2014**, *53*, 11203–11207; *Angew. Chem.* **2014**, *126*, 11385–11389; b) S.-i. Naya, T. Niwa, T. Kume, H. Tada, *Angew. Chem. Int. Ed.* **2014**, *53*, 7305–7309; *Angew. Chem.* **2014**, *126*, 7433–7437.
- [3] a) K. G. Stamplecoskie, P. V. Kamat, *J. Am. Chem. Soc.* **2014**, *136*, 11093–11099; b) Y. Xu, B. Zhang, *Chem. Soc. Rev.* **2014**, *43*, 2439–2450; c) S. Eustis, M. A. El-Sayed, *Chem. Soc. Rev.* **2006**, *35*, 209–217; d) A. Sobhani, M. W. Knight, Y. M. Wang, B. Zheng, N. S. King, L. V. Brown, Z. Y. Fang, P. Nordlander, N. J. Halas, *Nat. Commun.* **2013**, *4*, 1643; e) M. A. Mahmoud, M. A. El-Sayed, *J. Am. Chem. Soc.* **2010**, *132*, 12704–12710; f) L. Liu, S. Ouyang, J. Ye, *Angew. Chem. Int. Ed.* **2013**, *52*, 6689–6693; *Angew. Chem.* **2013**, *125*, 6821–6825.
- [4] a) S. Linic, P. Christopher, D. B. Ingram, *Nat. Mater.* **2011**, *10*, 911–921; b) M. L. Brongersma, N. J. Halas, P. Nordlander, *Nat. Nanotechnol.* **2015**, *10*, 25–34.
- [5] a) L.-B. Zhao, M. Zhang, Y.-F. Huang, C. T. Williams, D.-Y. Wu, B. Ren, Z.-Q. Tian, *J. Phys. Chem. Lett.* **2014**, *5*, 1259–1266; b) L. Brus, *Acc. Chem. Res.* **2008**, *41*, 1742–1749; c) A. Giugni, B. Torre, A. Toma, M. Francardi, M. Malerba, A. Alabastri, R. P. Zaccaria, M. I. Stockman, E. Di Fabrizio, *Nat. Nanotechnol.* **2013**, *8*, 845–852.
- [6] a) X. Chen, H.-Y. Zhu, J.-C. Zhao, Z.-F. Zheng, X.-P. Gao, *Angew. Chem. Int. Ed.* **2008**, *47*, 5353–5356; *Angew. Chem.* **2008**, *120*, 5433–5436; b) M. Haruta, A. Ueda, S. Tsubota, R. M. Torres Sanchez, *Catal. Today* **1996**, *29*, 443–447.
- [7] a) F. Wang, C. Li, H. Chen, R. Jiang, L.-D. Sun, Q. Li, J. Wang, J. C. Yu, C.-H. Yan, *J. Am. Chem. Soc.* **2013**, *135*, 5588–5601; b) M. Wen, S. Takakura, K. Fuku, K. Mori, H. Yamashita, *Catal. Today* **2015**, *242*, 381–385.
- [8] Z. Zheng, T. Tachikawa, T. Majima, *J. Am. Chem. Soc.* **2014**, *136*, 6870–6873.
- [9] a) S. K. Cushing, J. Li, F. Meng, T. R. Senty, S. Suri, M. Zhi, M. Li, A. D. Bristow, N. Wu, *J. Am. Chem. Soc.* **2012**, *134*, 15033–15041; b) W. B. Hou, S. B. Cronin, *Adv. Funct. Mater.* **2013**, *23*, 1612–1619; c) Z. Liu, W. Hou, P. Pavaskar, M. Aykol, S. B. Cronin, *Nano Lett.* **2011**, *11*, 1111–1116.
- [10] a) B. Dong, B. Cao, Y. He, Z. Liu, Z. Li, Z. Feng, *Adv. Mater.* **2012**, *24*, 1987–1993; b) J. Lee, N. A. Kotov, *Nano Today* **2007**, *2*,

- 48–51; c) K. Okabe, N. Inada, C. Gota, Y. Harada, T. Funatsu, S. Uchiyama, *Nat. Commun.* **2012**, *3*, 705.
- [11] M. Takase, H. Nabika, S. Hoshina, M. Nara, K.-i. Komeda, R. Shito, S. Yasuda, K. Murakoshi, *Phys. Chem. Chem. Phys.* **2013**, *15*, 4270–4274.
- [12] a) O. Neumann, A. S. Urban, J. Day, S. Lal, P. Nordlander, N. J. Halas, *ACS Nano* **2012**, *7*, 42–49; b) Z. Fang, Y.-R. Zhen, O. Neumann, A. Polman, F. J. García de Abajo, P. Nordlander, N. J. Halas, *Nano Lett.* **2013**, *13*, 1736–1742.
- [13] Y. F. Huang, M. Zhang, L. B. Zhao, J. M. Feng, D. Y. Wu, B. Ren, Z. Q. Tian, *Angew. Chem. Int. Ed.* **2014**, *53*, 2353–2357; *Angew. Chem.* **2014**, *126*, 2385–2389.
- [14] Z. Zheng, T. Tachikawa, T. Majima, *J. Am. Chem. Soc.* **2015**, *137*, 948–957.
- [15] “Probing the Local Temperature of Au NPs by Surface-Enhanced Raman Spectroscopy”: B. J. Liu, J. M. Feng, S. Hu, C. Zong, K. Q. Lin, X. Wang, D. Y. Wu, B. Ren, manuscript in preparation.
- [16] O. Neumann, C. Feronti, A. D. Neumann, A. Dong, K. Schell, B. Lu, E. Kim, M. Quinn, S. Thompson, N. Grady, P. Nordlander, M. Oden, N. J. Halas, *Proc. Natl. Acad. Sci. USA* **2013**, *110*, 11677–11681.

Received: June 30, 2015

Published online: August 17, 2015